

Motion Correction for Diffusion-Weighted Segmented EPI: Performance of an Iterative Parameter Space Searching Technique Evaluated with Numerically Simulated Motion Artifacts

J. D. Winter^{1,2}, N. Gelman^{1,2}, R. T. Thompson^{1,2}

¹Lawson Health Research Institute, London, Ontario, Canada, ²Medical Biophysics, University of Western Ontario, London, Ontario, Canada

Introduction:

Acquisition of diffusion-weighted (DW) images using segmented echo planar imaging (EPI), has advantages over the single shot EPI acquisition including reduced image distortion, blurring and acoustic noise levels. However, these images are often degraded by ghosting due to inter-segment phase differences generated by motion during the large diffusion gradients. To reduce ghosting artifacts, phase correction based on navigator echo signals is often performed.

It has also been demonstrated that phase corrections can be performed using an iterative parameter space search to determine the optimal phase correction values.¹ This technique was previously applied¹ to DW images ($b = 350 \text{ s/mm}^2$) obtained using two and four-segment interleaved EPI from a single subject. To investigate the potential of this technique with a larger number of segments using a “mosaic” (i.e., each segment is a k-space block) segmented EPI acquisition, the authors performed computer simulations in which motion degradation was introduced into a “simulated image” by perturbing the phase parameters of one segment. The standard deviation of the errors in the optimized values of the phase correction parameters was studied as a function of the signal-to-noise ratio (SNR).

In this current abstract we present the results of computer simulations to investigate the performance of this motion correction method, applied to interleaved segmented EPI, as a function of the level of image degradation. The interleaved acquisition scheme was investigated here rather than the “mosaic” as the latter scheme often suffers from periodic modulation of the k-space signal. The effects of motion during large gradients were simulated by perturbing the phase difference between all segments on an experimentally obtained non-diffusion weighted image acquired with an eight-segment acquisition.

Methods:

The numerical simulations were performed on one slice of a T2-weighted ($TE = 135 \text{ ms}$) segmented echo planar image that had been acquired, from a neonate as part of a MRI study of neonatal hypoxic ischemic encephalopathy. (Research ethics board approval and parental informed consent had been obtained). In addition, a diffusion-weighted image ($b = 600 \text{ mm}^2/\text{s}$) corresponding to the same slice was used to provide a SNR value for the simulations. The images had been acquired using a 3.0T MRI system. Imaging parameters included: 10 slices, 128×128 matrix, bandwidth = 100kHz, $FOV = 160\text{mm}$, $TR = 10 \text{ R-R cardiac intervals}$ (approximately 5s).

Image processing of the T2-weighted image prior to the motion simulations included (1) adding random noise to the image to reduce the SNR to a level corresponding to that of the diffusion weighted image (16:1) and (2) applying the motion correction algorithm to the resulting image to remove minor motion artifacts. To simulate motion artifacts in DWI using this base image, three phase parameters for each of seven segments were perturbed using a random number generator. The phase parameters are 0th order phase (ϕ), 1st order phase along the x direction (α) and 1st order phase along the y direction (β).

Motion simulations were first performed separately for each one of the three phase parameters. For ϕ , the random phase value generator was restricted to between $-\pi/2$ and $\pi/2$ and run 100 times. Incremental limits were used for α (± 0.005 to $\pm 0.25 \text{ rad/pixel}$, in 18 steps) and β (± 0.005 to $\pm 0.05 \text{ rad/pixel}$ in 10 steps) to provide a wide distribution of motion artifact levels. Lastly, motion simulations were applied by perturbing all three phase parameters simultaneously. In this case, incremental limits for both α and β were (± 0.005 to $\pm 0.05 \text{ rad/pixel}$ in 10 steps). To obtain roughly equivalent limits for ϕ , the ϕ limits (rad/pixel) were multiplied by the number of pixels from the center to the edge of the brain (30). Ten experiments were performed for each limit.

Motion correction was performed using a post-processing technique similar to that previously reported¹ and applied to 2 and 4 shot DWI EPI. However, we modified the search procedure to reduce post-processing time (two minutes for 8 segments). The procedure begins with a coarse search of the ϕ values for each segment, which provides starting point for the Gauss-Newton minimization of the ϕ , which in turn provides starting ϕ values for the next search involving both ϕ and α . This in turn provides ϕ and α start values for the final search of ϕ , α , and β . 1st order phase correction was applied using the refocusing reconstruction technique.³

The relative efficacy of the motion correction techniques were quantified using the artifact to signal ratio (ASR) defined by:

$$ASR = \frac{S_{GHOSTING} - S_{NOISE}}{S_{BRAIN}}$$

Where S_{BRAIN} is the mean signal from the brain, $S_{GHOSTING}$ is the mean signal in the background region displaced from the head in the phase encode direction and S_{NOISE} is the mean signal in the background region displaced from the head in the read direction. In addition, the accuracy of the algorithm was assessed by determining the difference between the optimized and true values of ϕ , α , and β for each of the seven perturbed segments (21 parameters). This was expressed as the root mean square over the 21 phase values.

Results:

For images in which the perturbation was applied only to the net phase (ϕ) the corrected images showed very small ASR values ($\approx 0.5\%$) independent of the ASR of the corrupted image (Fig. 1). However for cases where the perturbation was applied independently to α or β or to all three parameters (ϕ , α , and β), the ASR values for the corrected images increase as the ASR of the corrupted image increases (Figure 1). For the independent perturbations of ϕ , α , and β , the phase parameters were determined with high accuracy except for perturbations in α or β above a “breakdown point” (Table 1). For perturbations involving all three ϕ , α , and β , the breakdown point was similar to that for β perturbations only.

Discussion:

Our motion simulations demonstrated the effectiveness of this technique to correct for motion induced phase perturbations. Although rotational motion during the large gradients may also lead to drops in the signal amplitude associated with intra-voxel phase variation one might expect this effect to be reasonably small for first order phases variation less than the breakdown points demonstrated here (Table 1, e.g., 0.076 radians across one pixel). The algorithm breakdown point for β (0.015 rad/pixel from Table 1) corresponds to a k-space shift of approximately $\Delta k/3$, Δk where is the distance between two k-space lines. This is a reasonable limit given that a shift of Δk should be equivalent to loss of information from an entire image segment.

References:

1. Robson MD *et al*, MRM, **38**:82-88 (1997)
2. Miller KM *et al*, MRM, **50**:343-353 (2003)

Financial Support from the Canadian Foundation for Innovation (CFI), the Ontario Research and Development Challenge Fund (ORDCF), Multi-Magnetics Inc (MMI) and the Canadian Institutes of Health Research (CIHR) are gratefully acknowledged.

Phase	Breakdown rms phase	Error in rms phase before breakdown
ϕ	-	0.015 rad
α	0.076 rad/pixel	$1.6 \times 10^{-4} \text{ rad/pixel}$
β	0.015 rad/pixel	$1.1 \times 10^{-4} \text{ rad/pixel}$

Table 1. Accuracy of phase values determined by the search algorithm. Algorithm performs well for root mean square (rms) phase perturbations below a breakdown point.

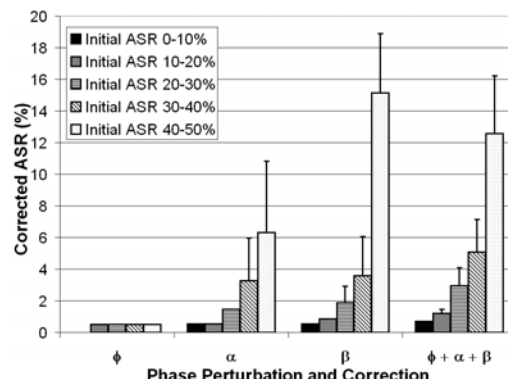


Figure 1. The corrected image ASR values for numerically simulated motion.